



HAL
open science

Creep of concrete during Alkali-Aggregates Reaction

Clément Lacombe, Thierry Vidal, Alain Sellier, Christine Noret, Patrice Anthiniac

► **To cite this version:**

Clément Lacombe, Thierry Vidal, Alain Sellier, Christine Noret, Patrice Anthiniac. Creep of concrete during Alkali-Aggregates Reaction. *Construction and Building Materials*, 2022, 336, pp.127355. 10.1016/j.conbuildmat.2022.127355 . hal-03696886

HAL Id: hal-03696886

<https://hal.insa-toulouse.fr/hal-03696886>

Submitted on 22 Jul 2024

HAL is a multi-disciplinary open access archive for the deposit and dissemination of scientific research documents, whether they are published or not. The documents may come from teaching and research institutions in France or abroad, or from public or private research centers.

L'archive ouverte pluridisciplinaire **HAL**, est destinée au dépôt et à la diffusion de documents scientifiques de niveau recherche, publiés ou non, émanant des établissements d'enseignement et de recherche français ou étrangers, des laboratoires publics ou privés.



Distributed under a Creative Commons Attribution - NonCommercial 4.0 International License

Creep of concrete during Alkali-Aggregates Reaction

Lacombe Clément^{a,b}, Vidal Thierry^a, Sellier Alain^a, Noret Christine^b, Anthinac Patrice^b

^a*LMDC, Université de Toulouse, INSA/UPS Génie Civil, 135 Avenue de Rangueil, 31077 Toulouse cedex 04 France.*

^b*TRACTEBEL Engineering, 5 Rue du 19 Mars 1962, 92230 Gennevilliers, France*

Abstract

The sustainability of operating hydropower schemes is an important issue in the context of ecologic-transition. However, some concrete dams are affected by Alkali-Aggregates Reaction (AAR), which can be a major concern for their safety. In the case of arch dams, where the overall stability is based on the transmission of stresses from the structure to the foundation, the swelling induced by the reaction can generate additional stresses. As concrete creeps under mechanical loading, a competition occurs between stress rising due to swelling and stress release due to creep. To capture this competition, the creep test must be led after a significant level of swelling and not before its initiation as often observed in lab tests. So, a new testing program has been developed to capture interactions between compressive creep and swelling induced by ongoing AAR. It was applied on two similar concretes differing one-another only by the reactivity of their aggregates. After one month of autogenous curing, concrete samples were immersed in sodium-hydroxide solution to accelerate the AAR. Once a significant part of the maximal free swelling is reached, they were sealed to keep the ongoing reaction, and a part of them were loaded uniaxially, while the others remained free of stress. The results show that 40% of the swelling occurring before the loading was rapidly erased in the compressed direction. Afterwards, similar creep evolutions were observed for reactive and non-reactive concretes, without any report of the swelling in the free directions for the reactive one, despite the ongoing of AAR.

Keywords: Lab-tests, Concrete, Alkali-Aggregates Reaction, Creep

1. INTRODUCTION

The sustainability of structures affected by the Alkali-Aggregates Reaction (AAR) is a major concern on many points. On the first hand, the integrity of dam must be ensured to protect the population downstream. On a second hand, keeping serviceability of existing concrete dams as long as possible allows to avoid the demolition and the reconstruction, and then limit the CO₂ emission. In the case of an arch dam, the AAR swelling can induce a change of the stress distribution in the structure and in its foundation, which could affect their interactions and possibly their stability.

The three main causes of this reaction development were identified in 1975 [1]. They are: alkali-sensitive aggregates, sufficient alkali-content and high moisture level in the concrete. This last one must exceed above 80% according to Larive [2]. For others, the swelling rate depends on the water saturation and starts at 30% [3, 4].

In 1997, Larive proposed a sigmoid (s-shaped) function to describe the free swelling induced by this reaction [5]. The study also defined a temperature dependence of the expansion velocity complying with an Arrhenius law.

In France, based on numerous studies on the reaction, recommendations [6] have been established to prevent the AAR in the new concrete structures. They classify the aggregates in three alkali-sensitive types (Reactive, Potentially Reactive and Non-Reactive), while the total alkali content limit is fixed at 3.5 kg/m³ of concrete.

The AAR swelling generates several effects on mechanical concrete behavior. A significant reduction of the modulus of elasticity occurs, while the compressive strength is less affected [5, 7, 8, 9, 10, 11, 12]. These effects on the mechanical properties have led some researchers to investigate the long term behavior of concretes subjected to sustained uniaxial compression [5, 7, 13, 14, 15, 16]. Some authors observed that, under a sufficiently high stress, swelling can stop [17, 18], but there is no statement about the report of swelling on the free directions. This vanishing effect

Email address: clement.lacombe@tractebel.engie.com
(Lacombe Clément)

of the compressive stress has been firstly reported in 1994 by Charlwood [19] from the observation on dams affected by the AAR. He proposed a directional logarithmic law linking the swelling rate and the applied stress where the vanishing limit was proposed at 8 MPa (1160 Psi). However, the influence of the reaction on the long term concrete behavior is still unknown or misunderstood. Until 2019, most of laboratories studies investigated the creep of the concrete loaded before the AAR starts, but none after a first stage of free swelling as it occurs in observed structures. Nevertheless, a recent research studied the creep behavior of various affected concrete at different stages of swelling progress. They concluded that the higher the reaction rate, the higher the creep velocity [11] Saouma and Perotti modeled swelling reduction in compressed direction assuming constant volume swelling, dispatched on the three main directions thanks to stress dependent factors [20]. Other authors proposed mesoscopic numerical modeling of concrete, where the cement matrix is a viscoelastic behavior material able to absorb swelling [21]. They assumed that the cement paste creep surrounding the aggregates is enough to absorb a part of overpressure caused by the reaction products. But this mesoscale numerical model cannot allow the calculation of massive structures. To avoid this limit to structures calculation, Grimal et al have established an analytical rheological model implemented in a finite elements software [22, 23].

In the arch dams subjected to the AAR, irreversible displacements of their crest in the upstream and vertical direction can be observed, and they are the visible consequences of swelling of the concrete. At the reaction initiation, the stresses are relatively low. After significant swelling, the concrete is subjected to additional stresses induced by restrained displacements. In this context, the loading appears while the reaction goes on. Rheinhardt et al [11] tried to capture this interaction, but in their test, the reaction stopped when the load was applied. Furthermore, only the axial strains were assessed, so no conclusions can be done about the report of the swelling in the unloaded directions.

The aim of this present work is the quantification of the consequence of ongoing AAR on the creep and on the swelling in the free directions. In order to have a comparative reference for the creep rate, the reactive concrete behavior is compared to an unaffected concrete designed to reach the same mechanical properties as the reactive one before the reaction. Each one was studied under uniaxial compressive load and in unloaded conditions. The monitoring of the two mixtures allowed to separate the influence of each phenomena, and specif-

ically the effect of the ongoing AAR on the creep behavior. The figure 1 schematizes the tests conditions and the global methodology. The longitudinal and the orthoradial strains were recorded to assess the potential report of swelling in the unloaded direction when AAR and creep are concomitant.

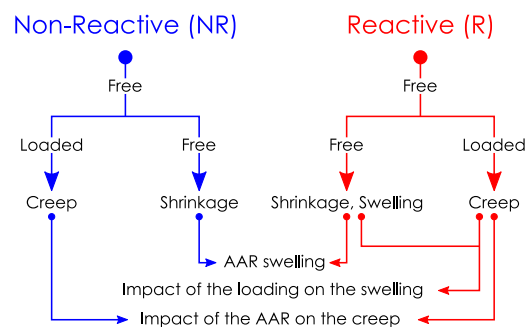


Figure 1: Global methodology of laboratory tests

The chronology of test was inspired by the on-site life of a concrete that can be found in a dam subjected to AAR. It can be divided in three stages:

- Stage 1: Autogenous curing to represent the concrete condition during the dam building;
- Stage 2: Immersion into the water to favorize the reaction, it is also a representative condition of the upstream of a dam during its operating phase;
- Stage 3: Uniaxial sustained loading representing the effect of the foundation reactions due to swelling. The creep test is launched when AAR swelling is significant. An autogenous condition is applied to maintain a high moisture content to allow the AAR to continue, and be representative of concrete behavior at the heart of the structure. In parallel, the behavior of unloaded specimens is observed.

2. EXPERIMENTAL TESTING PROGRAM

2.1. Aggregates

The Reactive concrete (R) and the Non-Reactive concrete (NR) mixes have been designed to differ only by the reactivity of their aggregates. This implies that the origins of aggregates, and thus their mineralogy and their mechanical properties are not similar, but they both contain a significant part of lime and their elastic properties are close.

The Non-Reactive (NR) aggregates were extracted from a limestone rock, and from a calcareous-siliceous

Table 1: Mechanical properties of the aggregates

Reactivity of the rock	Non-Reactive (NR) [24]	Potentially Reactive (PR)
Quarry's name	Boulonnais	Gaurain
Compressive strenght [MPa]	224 ± 25	178 ± 47
Young's modulus [GPa]	80 ± 2	78.6 ± 0.2
Poisson's ratio	0.31 ± 0.01	0.31 ± 0.02

rock for the Potentially Reactive (PR) ones. Their mechanical properties are given in table 1.

The mechanical properties of the non-reactive aggregates have been reported by Makani et al [24] while the potentially reactive ones were characterized during the study, in accordance with French standards [25, 26]. It was assessed on three cylindrical drilled rock specimens with a diameter of 58 mm and a height of 110 mm.

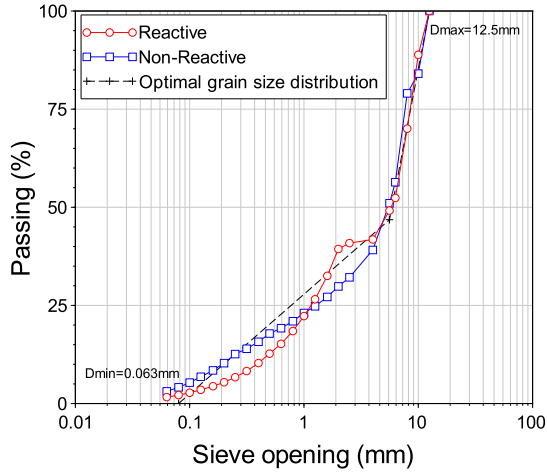


Figure 2: Particle size distribution of the reactive and the non-reactive aggregates

2.2. Concrete mixtures

The sand and the gravel used in the Non-Reactive mixes (NR) were only Non-Reactive aggregates (NR), while only Potentially Reactive aggregates (PR) were used in the Reactive mixes (R).

The particle size distributions of the reactive and non-reactive aggregates, sand and gravel, have been constructed to be close as possible to limit the effects of potentially differences of intergranular porosity on concretes mechanical behavior. In accordance with standards [27], the optimal grain size distribution was calculated for a maximal diameter of 12.5 mm and a minimal diameter of 0.063 mm, with a breaking point representing a passing of 46.8% in 5.6 mm sieve.

Aggregate distribution of the mix was close to the optimal grain size distribution as illustrated in figure 2. The difference in the sand-fine/gravel interval was the consequence of different grading curves of each kind of aggregate.

The concrete mixtures are presented in table 2. They were similar regarding the proportion of materials, with 1713 kg/m^3 of aggregates and 410 kg/m^3 of Ordinary Portland Cement (OPC) (CEM I 52.5 N CE PM-ES-CP 2 NF). An effective water/cement ratio of 0.46 was chosen to maintain the workability of the concrete during the casting, and to reach a compressive strength representative of usual dam concretes.

The Na_2O equivalent content was increased from 0.28% (cement content) to 1.25% of the cement mass to ensure the initiation of the AAR in the reactive concrete. It was done by adding sodium hydroxide in the mixing water of the two mixes. As a result, the total alkali content of the concrete was 5.125 kg/m^3 of concrete, which exceeded the limit value fixed by the French recommendations [6].

Table 2: Concrete mixes

Mix name	Non-Reactive (NR)	Reactive (R)
Components		
Sand	NR 0-2mm	680 kg/m^3
	PR 0-4mm	672 kg/m^3
Gravel	NR 4-12.5mm	1041 kg/m^3
	PR 4-6mm	190 kg/m^3
	PR 6-12.5mm	843 kg/m^3
Cement	410 kg/m^3	
Eff. Water/Cement	0.46	
Total alkali content	5.125 kg/m^3	

2.3. Tests chronology

- Stage 1: curing (28 days)

After casting, all the specimens were directly stored at $95\%(\pm 5\%) \text{ RH}$ and $20^\circ\text{C}(\pm 1^\circ\text{C})$. After one day, the samples were demolded and stored at $20^\circ\text{C}(\pm 1^\circ\text{C})$ in autogenous conditions in hermetic plastic bags until the date of 28 days from casting.

- Stage 2: immersion time (111 days)

After 28 days, all the specimens were immersed in 2.5 times their volumes of 1M hydroxide solution and kept at $38^{\circ}\text{C}(\pm 2^{\circ}\text{C})$. The heating allowed the increase of the reaction's velocity while the immersion prevented the leaching of alkalis, in accordance with previous studies [28, 29].

The specimens were stored in these conditions until the free AAR swelling strain reached the value of $300\ \mu\text{m}/\text{m}$ which represents 10% of the expected final free swelling. It also corresponds to the time when the swelling rate is maximum. This choice was done from a preliminary experimental program, whose results are presented in figure 3.

Once the swelling strain of $300\ \mu\text{m}/\text{m}$ is reached, all the samples were taken out of the solution and protected from desiccation by two layers of adhesive aluminum foils in order to be placed in creep cells room at $20^{\circ}\text{C}(\pm 1^{\circ}\text{C})$ and $50\%(\pm 5\%)$ RH.

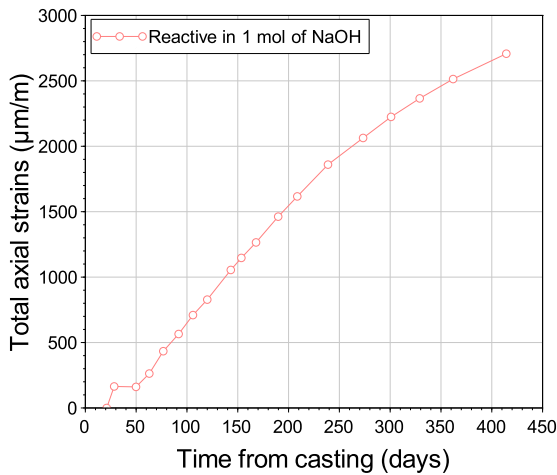


Figure 3: Free expansion of concrete mix with the reactive aggregates and immersed in a 1M NaOH solution at 38°C after 21 days of auto-genous curing

- Stage 3: long term experimentation (861 days)

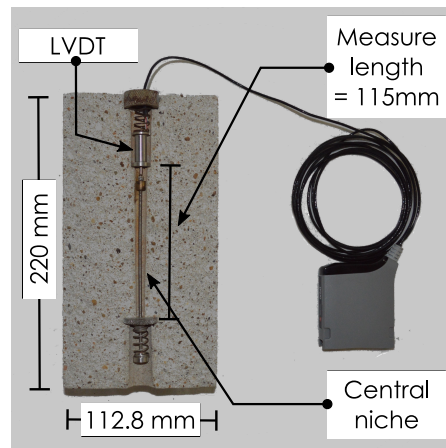
During this last stage, the sealed samples were stored at $20^{\circ}\text{C}(\pm 1^{\circ}\text{C})$. Half of them remained free to deform (stage 3.1) while the others were loaded with a constant uniaxial compressive stress (stage 3.2).

To avoid mechanical damage and be representative of stress level inducing creep on real structures, the loading stress value corresponded to 30% of the lowest compressive strength of the two concretes mixes assessed at

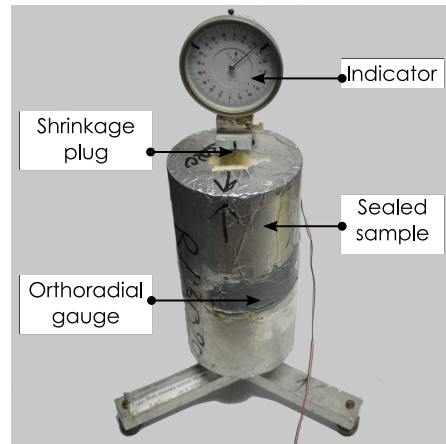
the end of the stage 2. It was applied using a jack linked to an hydraulic system where the pressure is sustained thanks to a nitrogen tank, in accordance with standards [30].

2.4. Specimens and measurements

For each mix, 11 cylinders with a diameter of 113 mm and a height of 220 mm were cast. From this panel, 3 were used to assess mechanical properties of sound concrete (Young's modulus and uniaxial compressive strength) at the beginning of the stage 2, and 3 others were used at the end of this stage.



(a) Inner LVDT sensor system



(b) Sealed sample equipped with shrinkage plugs and ortho-radial gauges installed on the indicator system

Figure 4: Pictures of the measurements systems

Before concrete casting, two samples molds were equipped by removal elements to create a central cylindrical niche to host an LVDT sensor to record longitudinal strain. This system is presented in the figure 4.a. It assesses the strains measurement on an axial length of 115

mm out of the fretting influence zone. This system allowed the strain monitoring of the samples during stage 1 from one day, and for the loaded samples during stage 3.

3 other samples were used to measure the uniaxial strain during the stage 2 and the stage 3 in the case of unloaded condition. Since LVDT sensors are not able to resist to the hydroxide solution immersion of stage 2, a second system of measurement had to be used. The longitudinal strain was obtained using an indicator measuring the relative variation of length of concrete samples equipped by stainless-steel plugs axially bonded on their level surfaces to ensure the contact with the indicator. This system is in accordance with standards [31] and is presented in figure 4.b.

To record the strains using indicator and the mass variations of the samples during the immersion stage 2, the specimens in the hydroxide solution were stored at $20^{\circ}\text{C}(\pm 1^{\circ}\text{C})$ the day before the measurements to slowly decrease the temperature samples, and thus avoid thermal strains and thermal damage in concrete. After the measurements, the samples in solution were re-placed at $38^{\circ}\text{C}(\pm 2^{\circ}\text{C})$ to slowly increase the temperature.

The orthoradial strain during the stage 3 has been measured on each sample thanks to two 12.5 mm length strain gauges, as presented in figure 4.b. They were placed diametrically opposed at the mid height of samples.

1000 days after the casting, the porosity and the water content were measured in accordance with the standards [32]. This test allowed to verify the sealing efficiency through the water content control.

3. RESULTS

3.1. Evolution of the mechanical properties

The mechanical properties of both concretes are presented in table 3. The first mechanical tests were performed after 35 days in autogenous conditions. They were done to verify the similarity of the mechanical properties of the two concrete mixes (NR and R) before the swelling initiation. At this date, a relative difference of 4.7% between the Young's modulus was observed. This value reached 13.9%, after the immersion. The difference at 35 days can be explained by a higher Young's modulus of the reactive aggregates than the non-reactive ones, as observed in the rock characterization presented in table 1. The increasing evolution is explained by two phenomena: from a side, the rise of the modulus of the non-reactive concrete due to the hydration, with a gain of 5.9% between the two dates; from another, a decrease

of the reactive concrete modulus due to the AAR with a loss of 4.3%. It is a consequence of micro-cracking in the cement paste as explained in previous other laboratory study [33].

The compressive strength is also impacted by AAR, but less. Indeed, the observed increase between the two dates for the non-reactive concrete and the reactive one, 24.1% and 15.8% respectively. It represents a difference of -8.2% between the two mixes, which is similar to the modulus one (-10.2%).

At 136 days corresponding to the date of creep tests launch, the compressive strength assessed on the non-reactive sample was the lowest, with a mean value of 56.2 MPa. In consequence, the sustained axial stress during the phase 3.1 corresponded to 30% of this strength, i.e. 17.1 MPa.

3.2. Water content and porosity at 1000 days

The porosities at 1000 days were 13.8% and 13.9% for the non-reactive and reactive concretes, respectively. The water saturation rates (volume of water / volume of porosity) were assessed thanks to this porosity test coupled with the mass evolution between the beginning and the end of the stage 3. Their values were 0.93 for the non-reactive mix and 0.92 for the reactive one.

3.3. Mass variation

The mass variation measured during the immersion time is plotted in percentage in figure 5. The curves correspond to the mean of three values while the color area delimited the minimal and the maximal values for each measure. The reactive concrete values are represented by red circles while the non-reactive ones by blue squares.

The mass variation evolution of the two concretes can be separated in two steps. The first one, which occurs just after the first immersion, corresponds to the major part of the total mass gain and its kinetic is high. It is due to capillary absorption of water in concrete porosity until saturation. The second step corresponds to a slower mass gain, which is the consequence of the smallest porosity filling due to long time immersion.

The mass gain due to the capillary absorption is equivalent for the two concrete mixes revealing a similar porosity that was confirmed by the porosity test at 1000 days. A different mass variation can be observed from the outset of the second step, with a mass gain twice more important for the non-reactive samples than the reactive ones. It can be explained by the time needed to install the measurement systems the day after the casting, which was a little bit longer for the non-reactive

Table 3: Evolution with time of compressive strength and Young's modulus of each concrete mix and comparison with the relative difference between the two mixtures at the same date (3 Samples per mix and date)

Mix name	Non-Reactive	Reactive	Relative spread
Compressive Strength [MPa]			
End of the cure (35 days)	45.3 ± 1.2	51.1 ± 0.6	+12.8%
End of the immersion (136 days)	56.2 ± 1.0	59.2 ± 0.9	+5.3%
Evolution between the two dates	+24.1%	+15.8%	-8.2%
Young's modulus [GPa]			
End of the cure (35 days)	39.3 ± 0.3	37.5 ± 0.5	-4.7%
End of the immersion (136 days)	41.7 ± 0.3	35.9 ± 0.2	-13.9%
Evolution between the two dates	+5.9%	-4.3%	-10.2%

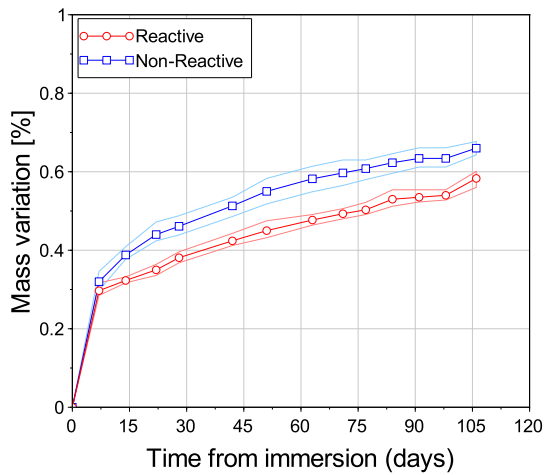


Figure 5: Mass variation of the two mixes during the immersion time

specimens. So, the non-reactive was slightly more desaturated at the beginning of the immersion stage, inducing in return, a higher mass gain during the following immersion stage.

From 15 days to the end of immersion, the behavior of the two concretes was similar in terms of mass variation. This time corresponded to an increase of 0.272% for the non-reactive samples while this valued was 0.260% for the reactive ones. After 70 days in solution, as the mass variation rate decreases, the porosity of the two concretes can be assumed to be saturated.

As a consequence, from 15 days, the difference of strains between the reactive and non-reactive specimens will be attributed to AAR.

3.4. Evolution of the axial strains

The evolutions of axial strains are presented in figure 7. The experimental stages captioned in figure 6 are represented in the upper drawers. The strains evolutions

are recorded from 1 day after casting to the end of experimentation (figure 7). They are plotted in sub-figure 7.a for the specimens in free swelling conditions, and figure 7.c for the ones loaded at 139 days. The reactive concrete is drawn with red circles while blue squares were used for the non-reactive one.

The lower graphs (figures 7.b and 7.d) represent the difference between the two curves above, and these strain evolutions can be considered as the swellings induced by AAR. In agreement with the mass variation of figure 5), they began at the end of capillary absorption stage, i.e. 15 days after the immersion that corresponds to 42 days after casting. The lighter curves represent the discrepancy of values. In the following part, the different stages of the test are commented.

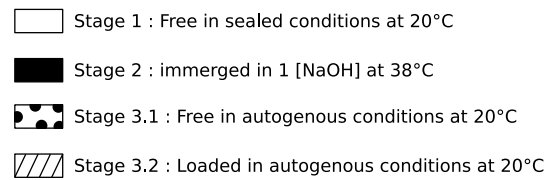


Figure 6: Exposure and loading conditions representation

3.4.1. Stage 1: Autogenous shrinkage during curing (from 1 to 28 days)

At the end of the curing period, the autogenous shrinkage reached $178 \pm 3 \mu\text{m}/\text{m}$ and $206 \pm 28 \mu\text{m}/\text{m}$ for the non-reactive concrete and reactive concrete, respectively. Regarding the Water/Cement ratio, the reported autogenous shrinkage at 28 days seems higher than usual. It may be attributed to the high alkali content. According to the assumption proposed by Inam and Skalny [34], a high content in alkali increases the hydration rate of the cement, and as a consequence the autogenous shrinkage.

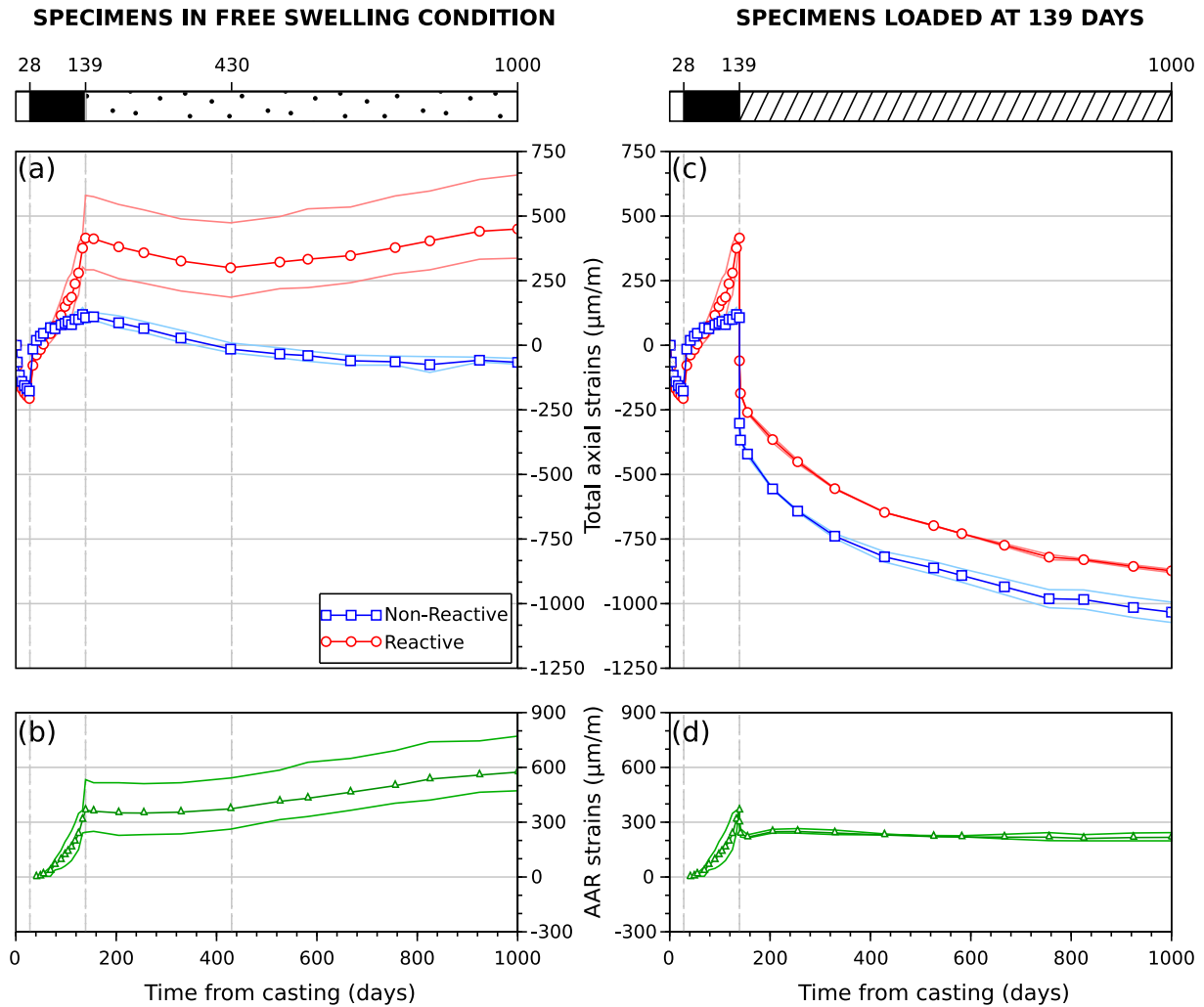


Figure 7: Evolutions of axial strains from 1 day after casting for free and loaded specimens

3.4.2. Stage 2: Free deformations during immersion (from 28 to 135 days)

Just after the immersion, a swelling due to the capillarity water absorption has been observed for the two concrete mixtures. After 14 days in hydroxide solution, these swellings reached the value of $197 \mu\text{m}/\text{m}$ for the non-reactive mix and $171 \mu\text{m}/\text{m}$ for the reactive one. This represents a relative difference of 13% that is similar to that observed between the mass variations at the same date.

Once swelling due to the capillarity water absorption ended, a small swelling is still observed. It is the consequence of porosity filling as observed on the mass variation evolution during the same period in figure 5. For the reactive curve, a swelling due to the AAR is clearly

discernible from 42 days after casting (figures 7.a and 7.c).

From this date, the difference between the two curves corresponds to AAR swelling as represented in figures 7.b and 7.d. The threshold of 0.03% was reached at 38°C . At this date, the swelling strain was $314 \mu\text{m}/\text{m}$ and the samples were taken out from the solution and protected from drying.

During the sealing time, despite an inevitable drying due to the preparation of specimens for sealing conditions, the reaction continued. Indeed, the shrinkage measured on the non-reactive specimens was $-12 \mu\text{m}/\text{m}$, while in a same time, the swelling of the reactive ones was $39 \mu\text{m}/\text{m}$.

At the end of the stage 2, the total strain reached the

values of $107 \mu\text{m}/\text{m}$ and $416 \mu\text{m}/\text{m}$ for the non-reactive concrete and the reactive ones, respectively, representing a AAR free swelling of $366 \mu\text{m}/\text{m}$.

3.4.3. Stage 3: Strains evolution during the long term experimentation in autogenous condition (from 139 to 1000 days)

- Stage 3.1: Free strains

During the first half time of the stage 3, a similar shrinkage is observable in figure 7.a on all the unloaded specimens of both concretes. From 139 to 430 days since casting, the shrinkage strain was $123 \mu\text{m}/\text{m}$ for the reactive mix and $116 \mu\text{m}/\text{m}$ for the non-reactive one. In the second part of the stage, the shrinkage of the non-reactive concrete continued but its rate decreased, while a swelling of the reactive concrete was observed, revealing a predominance of the AAR compared to the shrinkage. At this stage, the strong influence of water saturation and temperature on the strain rates can be noted.

At the end of the test program (figure 7.a), the total shrinkage reported for the non-reactive samples reached a value of $173 \mu\text{m}/\text{m}$ from the beginning of the stage 3. It was the consequence of inevitable drying through the sealing, which was confirmed by estimated water content at 1000 days, similar the both mixtures. These final similar values lead to assume that a same undesirable drying shrinkage occurred in all the specimens during the stage 3, in autogenous condition. As this drying stays rather low, the moisture remains sufficiently high to allow the AAR to continue. The latency of the AAR evolution observed at the beginning of stage 3 (figure 7.b) is linked to the change of moisture condition added to the temperature one [4, 5].

At 1000 days, the reaction was significantly slowed down due to the concrete desaturation. The final swelling value was $574 \mu\text{m}/\text{m}$, that represents a fifth of the total free swelling potential presented in figure 3.

- Stage 3.2: Time-dependent strains in autogenous conditions

After 139 days unloaded, the samples equipped with an inner sensor were loaded with a constant vertical compressive stress of 17.1 MPa (figure 7.c). This value corresponded to 30% of the compressive strength assessed on the non-reactive samples at the end of the immersion (cf table 3).

The elastic strain induced by the loading was $410 \mu\text{m}/\text{m}$ for the non-reactive mix and $476 \mu\text{m}/\text{m}$ for the reactive one. Reported on the AAR free swelling, this difference of $66 \mu\text{m}/\text{m}$ represented 18% of the free

AAR swelling evaluated at the same date. It can be assumed that this strain difference is the consequence of a partial re-closing of the micro-cracks induced by the AAR.

During the first 15 days after the loading (figure 7.d), the strain difference between the two mixes decreased from $366 \mu\text{m}/\text{m}$ at 139 days to $282 \mu\text{m}/\text{m}$ at 155 days after the casting. A higher delayed strain under loading evaluated at $81 \mu\text{m}/\text{m}$ was observed on the reactive samples compared to the non-reactive ones (figure 7.c). It could be due to a delayed re-closing of AAR micro-cracks.

After 15 days under constant load, the delayed strains evolutions of the two kinds of concrete were parallel, as illustrated in figure 7.c. It corresponded to a same creep kinetic for reactive and non-reactive concretes. Between 155 and 1000 days, the longitudinal delayed strain was $612 \mu\text{m}/\text{m}$ for the non-reactive mix while it reached the value of $614 \mu\text{m}/\text{m}$ for the reactive concrete. This similarity of creep kinetics implies that swelling in loaded direction has been stopped due to a load higher than the vanishing limit of 8 MPa observed by Charlwood [19], despite of the AAR continuation proven by the swelling of free samples and the evolution of radial strain shown in figure 8.

These results are in accordance with the experimental observations of Rheinhardt et al [11]. Their results also showed vanishing of the AAR swelling in the loaded direction that occurred during the two first weeks after the loading application. After this period, the delayed behavior of their concretes was similar, whatever the ongoing AAR at the loading date.

3.5. Evolution of orthoradial strains

The delayed orthoradial strains are presented in figure 8 with the same axis scale, sign convention and curve representations than the axial strains graphs in figure 7.

The Poisson's ratios were evaluated during the loading of the inner-sensor specimens. They were 0.20 and 0.24 for the non-reactive mix and the reactive one, respectively, as shown in figure 8.c.

After 260 days from casting, the difference between the radial strains of the two compositions restart, proving that AAR goes on. More, the radial swelling of reactive concrete ($127 \mu\text{m}/\text{m}$) was rather the same for both loaded and unloaded specimens, showing that uniaxial stress does not change the radial swelling for these test conditions.

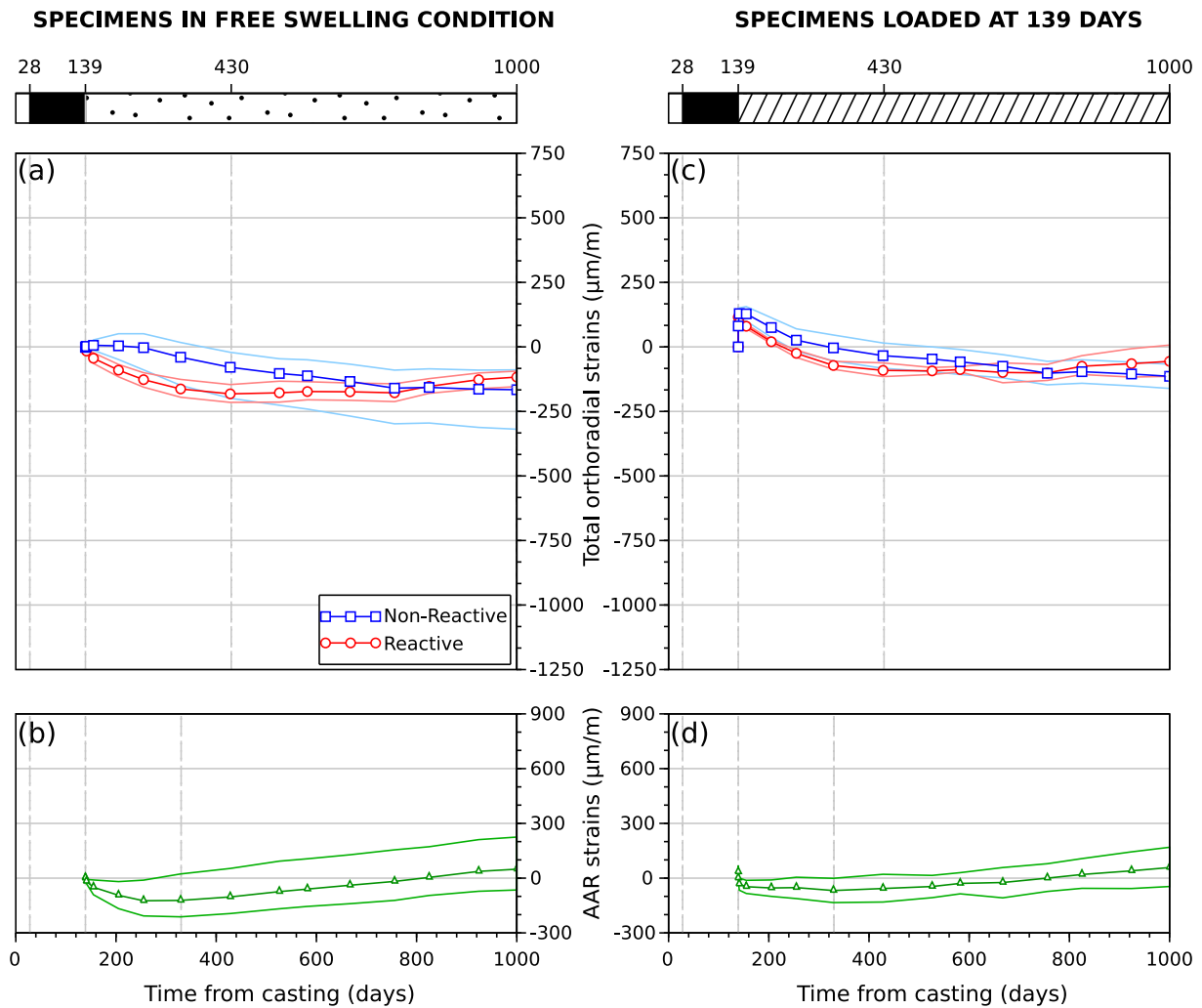


Figure 8: Delayed orthoradial strains for free and loaded specimens during the stage 3

4. CONCLUSION

By studying the long term behavior of two concretes that are initially close in terms of mechanical properties but not in terms of reactivity of aggregates, the effects of the ongoing AAR on the creep has been assessed, and the anisotropy of the swelling under uniaxial compression observed. The main conclusions are the following:

- For a small swelling of 0.03%, a loss of 10% of mechanical performances is measured;
- The decreases of the temperature and of the water saturation significantly reduce the kinetic of the AAR;
- The AAR can continue slowly in autogenous condition, provided that the initial water content in the porosity stays high enough;
- The AAR swelling of a reactive concrete was stopped in the loaded direction by the compressive stress of 17 MPa (30% of the compressive strength), and 40% of the initial free swelling can be resorbed in this direction;
- After two weeks under loaded, the long term creep rate of the reactive concrete is similar to that of the non-reactive concrete;
- For an initial small swelling of 0.03%, the impeded swelling in the loading direction was not reported

in the orthogonal free to swell directions.

5. ACKNOWLEDGMENT

This research was financially supported by Tractebel engineering France in collaboration with the LMDC Toulouse. Toulouse Tech Transfer (TTT) is gratefully acknowledged for the help during the set-up of the experimental program and for the preliminary studies. The test program has also been permitted thanks to the providing of some materials by the quarries of Gaurain and Boulonnais, which are gratefully acknowledged by the authors.

References

- [1] S. Diamond, A review of alkali-silica reaction and expansion mechanisms I. alkalis in cements and in concrete pore solutions, *Cement and Concrete Research* 5 (4) (1975) 329–345. doi:10.1016/0008-8846(75)90089-7.
- [2] C. Larive, A. Laplaud, O. Coussy, M. A. Berube, B. Fournier, B. Durand, The role of water in alkali-silica reaction, in: *Proceedings of the 11 th International Conference on Alkali-silica Reaction in concrete*, CRIB, 2000, pp. 61–70.
- [3] P. Morenon, S. Multon, A. Sellier, E. Grimal, H. François, E. Bourdarot, Impact of stresses and restraints on asr expansion, *Construction and Building Materials* 140 (2017) 58–74. doi:10.1016/j.conbuildmat.2017.02.067.
- [4] S. Poyet, Étude de la dégradation des ouvrages en béton atteints par la réaction alcali-silice : approche expérimentale et modélisation numérique multi-échelles des dégradations dans un environnement hydro-chemo-mécanique variable, Ph.D. thesis, Université de Marne la Vallée (2003).
- [5] C. Larive, Apports combinés de l'expérimentation et de la modélisation à la compréhension de l'alcali-réaction et de ses effets mécaniques, Ph.D. thesis, Ecole Nationale des Ponts et Chaussées (1997).
- [6] Concrete - provisions for the prevention of alkali silica reactions, FD P18-464, French Provisions (April 2014).
- [7] A. L. Roux, E. Massieu, B. Godart, Evolution under stress of a concrete affected by aar - application to the feasibility of strengthening of a bridge by prestressing, in: *Proceedings of the 9 th International Conference on Alkali-silica Reaction in concrete*, Concrete Society, 1992, pp. 599–606.
- [8] N. Smaoui, Contribution à l'évaluation du comportement structural des ouvrages d'art affectés de réaction alcali-silice (ras), Ph.D. thesis, Faculté des Sciences et de Génie de l'Université de Laval (2003).
- [9] O. Na, Y. Xi, E. Ou, V. E. Saouma, The effects of alkali-silica reaction on the mechanical properties of concretes with three different types of reactive aggregate, *Structural Concrete* 17 (1) (2016) 74–83. doi:10.1002/suco.201400062.
- [10] O. Mielich, H. W. Reinhardt, H. Özkan, Strength and deformation properties of alkali-silica reaction (asr) damaged concrete exposed to external alkalis, *Key Engineering Materials* 711 (2016) 665–672. doi:10.4028/www.scientific.net/KEM.711.665.
- [11] H. W. Reinhardt, H. Özkan, O. Mielich, Creep of concrete as influenced by the rate of expansion due to alkali-silica reaction, *Structural Concrete* 20 (5) (2019) 1781–1791. doi:10.1002/suco.201900133.
- [12] A. Mohammadi, E. Ghiasvand, M. Nili, Relation between mechanical properties of concrete and alkali-silica reaction (asr); a review, *Construction and Building Materials* 258 (119567) (2020). doi:10.1016/j.conbuildmat.2020.119567.
- [13] C. Gravel, G. Ballivy, K. Khayat, M. Quirion, M. Lachemi, Expansion of aar concrete under tri-axial stresses: simulation with instrumented concrete blocks, in: *Proceedings of the 11 th International Conference on Alkali-silica Reaction in concrete*, CRIB, 2000, pp. 959–968.
- [14] S. Multon, F. Toutlemonde, Effect of applied stresses on alkali-silica reaction-induced expansions, *Cement and Concrete Research* 36 (5) (2006) 912–920. doi:10.1016/j.cemconres.2005.11.012.
- [15] M. Berra, G. Faggiani, T. Mangialardi, A. Paolini, Influence of stress restraint on the expansive behaviour of concrete affected by alkali-silica reaction, *Cement and Concrete Research* 40 (9) (2010) 1403–1409. doi:10.1016/j.cemconres.2010.05.002.
- [16] C. Dunant, K. Scrivener, Effects of uniaxial stress on alkali-silica reaction induced expansion of concrete, *Cement and Concrete Research* 42 (2012) 567–576. doi:10.1016/j.cemconres.2011.12.004.
- [17] A. Giorla, Modelling of alkali-silica reaction under multi-axial load, Ph.D. thesis, École Polytechnique Fédérale de Lausanne (2013).
- [18] J. Liaudat, I. Carol, C. M. López, V. E. Saouma, Asr expansions in concrete under triaxial confinement, *Cement and Concrete Composites* 86 (2018) 160–170. doi:10.1016/j.cemconcomp.2017.10.010.
- [19] R. Charlwood, A review of alkali-aggregate reactions in hydroelectric plants and dams, *Hydropower Dams* 1 (1994) 77–80.
- [20] V. Saouma, L. Perotti, Constitutive model for alkali-aggregate reactions, *ACI Materials Journal* 103 (3) (2006) 194–202. doi:10.14359/15853.
- [21] A. Giorla, K. D. C. Scrivener, Influence of visco-elasticity on the stress development induced by alkali-silica reaction, *Cement and Concrete Research* 70 (2015) 1–8. doi:10.1016/j.cemconres.2014.09.006.
- [22] E. Grimal, A. Sellier, Y. Le Pape, E. Bourdarot, Creep, shrinkage, and anisotropic damage in alkali-aggregate reaction swelling mechanism-part I: A constitutive model, *ACI Materials Journal* 105 (2008) 227–235.
- [23] E. Grimal, A. Sellier, Y. Le Pape, E. Bourdarot, Creep, shrinkage, and anisotropic damage in alkali-aggregate reaction swelling mechanism-part II: Identification of model parameters and application, *ACI Materials Journal* 105 (2008) 236–242.
- [24] A. Makani, T. Vidal, G. Pons, G. Escadeillas, Time-dependent behaviour of high performance concrete: Influence of coarse aggregate characteristics, in: *Proceedings of the 14th International Conference on Experimental Mechanics*, EDP Sciences, 2010, pp. 3002–3010. doi:10.1051/epjconf/20100603002.
- [25] Rock - determination of the uniaxial compressive strength, NF P94-420, French Standard (December 2002).
- [26] Rock - determination of the Young modulus and the Poisson ratio, NF P94-425, French Standard (April 2002).
- [27] Tests for geometrical properties of aggregates - part 1 : determination of particle size distribution - sieving method, NF EN 933-1, European Standard (May 2012).
- [28] H. Brouwers, R. vanEijk, Alkali concentrations of pore solution in hydrating opc, *Cement and Concrete Research* 33 (2) (2003) 191–196. doi:10.1016/S0008-8846(02)01022-0.
- [29] M. Bérubé, J. Ollivier, G. Ballivy, Decrease of pore solution alkalinity in concrete tested for alkali-silica reaction, *Materials and Structures* 40 (2007) 909–921. doi:10.1617/s11527-006-9191-z.
- [30] Testing hardened concrete - part 17 : determination of creep of

- concrete in compression, NF EN 12390-16, European Standard (October 2019).
- [31] Testing hardened concrete - part 16 : determination of the shrinkage of concrete, NF EN 12390-16, European Standard (October 2019).
- [32] Concrete - testing hardened concrete - testing porosity and density, NF P18-459, French Standard (March 2010).
- [33] M. B. Haha, E. Gallucci, A. Guidoum, K. L. Scrivener, Relation of expansion due to alkali silica reaction to the degree of reaction measured by sem image analysis, *Cement and Concrete Research* 37 (8) (2007) 1206–1214. doi:10.1016/j.cemconres.2007.04.016.
- [34] J. Inam, J. Skalny, Alkalies in cement: A review: Ii. effects of alkalies on hydration and performance of portland cement, *Cement and Concrete Research* 8 (1) (1978) 37–51. doi:10.1016/0008-8846(78)90056-X.